Joint Power Allocation and Phase Shifts Design for Distributed RIS-assisted Multiuser Systems

Zhen Chen, *Senior Member*, *IEEE*, Gaojie Chen, *Senior Member*, *IEEE*, Xiu Yin Zhang, *Fellow, IEEE,* Jie Tang, *Senior Member, IEEE*, Shi Jin, *Fellow, IEEE,* Kai-Kit Wong, *Fellow, IEEE* and Jonathon Chambers, *Fellow, IEEE*

***Abstract*—Distributed reconfigurable intelligent surfaces (RISs) provide rich macro-diversity coverage due to different locations of the RISs, which is beneficial to combat coverage holes. However, the system performance relies on the effective coordination of multiple RISs. In particular, distributed RIS-assisted power allocation and the phase shifts of RISs should be jointly designed under nonlinear scheduling constraints. Thus, the resource allocation scheme for distributed RIS-assisted multiuser system is a crucial challenge. To tackle these issues, joint power allocation, phase shifts and communication scheduling design for distributed RIS-assisted systems is investigated in this paper, where all RISs simultaneously and cooperatively serve multiple users. To overcome the formulated nonconvex optimization problem, the original problem is decoupled into three subproblems and solved in an iterative manner. Specifically, we first consider the subproblem of power allocation, which can be solved via maximizing the ergodic achievable rate. By applying the ergodic rate, an approximate closed-form solution is formed for the power allocation. Subsequently, the phase shifts are optimized using the minimization-maximization optimization methods. Finally, a communication scheduling scheme is presented to address the scheduling variables. Numerical simulations are conducted to demonstrate that the considered solution outperforms the existing benchmark and achieves a near-optimal spectral efficiency.**

***Index Terms*—Distributed reconfigurable intelligent surfaces (RISs), power allocation, multiuser MIMO, phase shifts**

I. Introduction

THE rapid growth of the Internet-of-Things (IoT) has significantly increased the number of wireless devices. This expansion has also spurred the development of various smart applications, including automatic manufacturing, virtual reality, smart homes, and smart cities [1]. These advancements have introduced new challenges to support the low-latency communication, ultra-high capacity and massive connectivity requirements [2]. However, this increasing demand for ubiquitous connectivity and high data rates inevitably brings challenges, particularly in the form of high-energy consumption in next-generation wireless communication systems. To support the huge amount of data traffic, a mass of base stations (BSs) and mobile equipments will be required to be deployed in existing network infrastructure. However, massive antenna array architectures for BSs will significantly increase the implementation complexity and the associate hardware [3]. Particularly, the deployment of massive antenna arrays requires a significant number of radio frequency (RF) chains, which can lead to increased energy consumption and higher hardware costs.

To address above challenges, reconfigurable intelligent surface (RIS)-assisted wireless communication has been extensively studied as a cost-effective alternative [4]–[7]. RIS is capable of achieving unprecedented high throughput of system to against severe blockage scenarios [6]. Unlike conventional active beamforming or relaying technologies, each reflecting element of a RIS can dynamically adjust the direction of the reflected incident signals, thereby improving the communication quality of the desired propagation paths [8]–[11]. Moreover, due to the low hardware cost of the reflecting elements, RIS can be easily deployed in various wireless network scenarios, including, but not limited to, light communication [12], security communication [13] and wireless powered communication networks (WPCN) [14]. Notably, as highlighted in [9], the use of RIS allows the number of receive/transmit antennas required at the BS to be reduced to half of what is needed in conventional resource allocation approaches without RIS, significantly lowering hardware costs. To reap this benefit, it is natural to study the resource allocation scheme in RIS-assisted systems, which can greatly increase the service range and satisfy the quality of service (QoS) requirement to realize green communications.

There have been many reports regarding resource allocation maximization problems in RIS-assisted networks [15]–[19]. In [15], a RIS-assisted WPCN was exploited, where the optimal phase shifts were determined by using the iterative optimization scheme. Similarly, in [17], the authors tackled the joint power and spectrum allocation problem alongside RIS reflecting element design to maximize the sum-rate capacity in RIS-aided vehicle-to-everything (V2X) communication systems, employing a three-stage heuristic algorithm to find the achievable solution. Moreover, in [20], a RIS-assisted symbiotic radio system was examined, where joint beam training and power allocation optimization was applied to enhance the EE of the system. Building on this, a mathematical framework was proposed in [21] to jointly optimize the system's sum mean squared error, particularly addressing the non-line-of-sight (NLOS) propagation challenges with RIS playing a critical role.

Furthermore, the authors in [22] investigated an offset learning based deep learning scheme in RIS-assisted communication, where a viable solution was considered to achieve a good trade-off between the light-of-sight (LOS) and NLOS channels. In [23], the achievable weight SE optimization of the RIS-assisted cognitive radio network was investigated, which allows the decoupling of the reflection coefficients and

transmit power the constraints. To improve SE and EE in narrowband and broadband RIS-assisted systems, joint reflecting element and hybrid beamforming designs were proposed in [24], leveraging the angular sparsity of frequency-selective channels. Considering the QoS requirements of users, the transmit power control of the BS was studied with recommendations on the RIS deployment [25]. In [26], a penalty-based solution was developed to solve the power minimization problem, where the perfect and imperfect CSI were considered. To further provide low power consumption, authors in [27] investigated the energy-efficient power allocation scheme for heterogeneous small cell networks. Considering the interference of multipath fading channels, the authors in [28] developed a joint spectrum reuse, power allocation and interference suppression design in RIS-assisted device-to-device (D2D) communication, in which passive beamforming using RIS was employed to suppress the severe interference and enhance the desired communication coverage. Furthermore, by exploiting the full reflection properties of the RIS, several power allocation iteration algorithms in a RIS-assisted multiuser network were extensively studied, which include SE maximization in [29], [30], deep reinforcement learning in [31], and robust optimization in [32]. These solid contributions suggested that power allocation can bring appreciable gains for a RIS-assisted system.

However, the above works on resource allocation focus mostly on *single* RIS-assisted systems. As RIS-assisted systems evolve, the coverage regions of cellular networks continue to extend to meet the high-throughput, high-connectivity or various kinds of QoS demands, which will facilitate a growing number of RISs to be integrated in micro/femto-cellular networks. In particular, multiple RISs can provide richer macro-diversity. By distributing RISs over a large area, spatial diversity is enhanced, as the same information can be transmitted from fully uncorrelated RIS nodes to the receiver. This distributed setup effectively increases the likelihood of reliable signal reception, especially in challenging propagation environments. Therefore, multiple RISs (or distributed RISs) cooperation relations are no longer negligible. To further unlock the potential of cooperative RISs, distributed RISs were investigated to establish the cooperative reflection of the system, including perfect and imperfect timing synchronization among the RISs [33], [34]. Furthermore, the authors in [35] and [36] focused on multiple RIS-aided communication, in which the statistical characterization of the channel was derived by exploiting a Gamma or Log-Normal distribution. However, existing research works on multiple RIS-assisted networks neglect the communication scheduling among multiple RISs. This is a weakness as future IoT should support the connectivity of a massive number of energy-constrained terminals. These observations demonstrate that distributed RISs are very important in optimizing system performance, particularly to provide more robustness to the effect of the shadowing fading channel. However, increasing the physical size of the RIS module presents practical challenges in certain scenarios. This limitation arises due to space constraints and deployment feasibility. To address these challenges, researchers have introduced the concept of active RISs. Active RISs overcome the performance bottleneck caused by the multiplicative fading effect. They achieve this by incorporating active elements that amplify the signal, improving overall system performance. Unlike passive RIS, which only reflects signals, active RIS integrates amplification circuits to both direct and amplify reflected signals. This makes active RIS a popular research topic in wireless communications for enhancing system performance [37].

Furthermore, distributed RIS offers a mobility degree of freedom (DoF) to enhance the performance of wireless networks. However, each user may received signals from RISs at different locations with various propagation paths. Moreover, each RIS is subject to different and independent degree of large-scale fading effects, which results in a further complication involving communication scheduling and power allocation. In addition, due to the introduction of the distributed RIS, the power allocation is coupled together with communication scheduling of the multiple RISs, which makes it impossible to apply existing approaches directly. Therefore, research on distributed RIS-assisted systems for communication scheduling and power allocation are lacking.

Despite the extensive research on RIS-assisted multiuser systems, the joint design of communication scheduling and power allocation for distributed RIS scenarios has not been addressed in the existing literature, to the best of our knowledge. To bridge this gap, this paper incorporates communication scheduling constraints into the power allocation design for distributed RIS-assisted multiuser systems. The main contributions of this work are summarized.

- We investigate the distributed RIS-assisted multiuser scenario, taking into account practical limitations such as reflection coefficients and link capacity at various RIS locations. In such a system, multiple RISs are connected to a CPU. This configuration not only helps cover dead spots but also enhances spatial diversity by transmitting the same information through fully uncorrelated channels to the receiver.
- To enable distributed RIS-assisted multiuser systems, a joint power allocation, phase shifts and communication scheduling optimization scheme is proposed, in which an approximate closed-form and computationally tractable formula are provided to guarantee the achievable SE of the system. Based on the proposed design criteria, explicit cost functions are formulated to derive the solution, and its convergence and computational complexity are also analyzed.
- To address the non-convex optimization problem, a decoupling scheme is adopted, breaking the original maximization problem into three manageable subproblems: power allocation, phase shifts, and communication scheduling. In the power allocation design stage, a linear approximation using a series expansion is derived, followed by the application of an iterative sequential relaxation programming algorithm to solve the subproblem. For the phase shifts of multiple RISs, optimization is achieved through a combination of the minimization-maximization approach and successive convex approximation. Finally, the communication scheduling subprob-

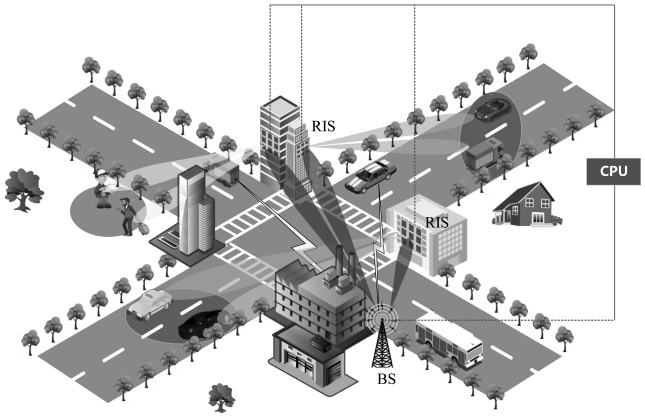

Fig. 1. A distributed RIS-assisted multiuser system.

lem is divided into two scalar continuously differentiable functions, which are solved sequentially to ensure a practical solution.

- Numerical results are conducted to verify the feasibility and robustness of the proposed scheme. Moreover, the convergence of the developed iterative algorithm for joint power allocation, phase shifts and communication scheduling optimization is also validated. With various practical setups, the achievable performance of the proposed algorithm against exsiting heuristically designed benchmarks are validated, and new insights on distributed RIS-assisted multiuser systems are also drawn.

The rest of the paper is organized as follows. In Section II, the system model and the problem formulation are described, in which multiple RISs incorporated into the multiuser system. In Section III, the joint distributed RIS-assisted phase shifts and power allocation optimization problem are considered, and then the SRM-based alternating optimization algorithm is introduced. Numerical results for evaluating the performance of the proposed scheme are provided in Section IV. Finally, conclusions are drawn in Section V.

II. Problem Formulation

As illustrated in Fig. 1, a BS equipped with n antennas communicates with single-antenna destination users, where all K users are served simultaneously by the RISs using the same time-frequency resource. In the distributed RIS-assisted multiuser system, full synchronization is maintained to ensure efficient operation. Additionally, each RIS is connected to a CPU via reliable, high-speed wireless links. The CPU is responsible for centralized tasks, including three-dimensional beamforming design, scheduling, and power allocation.

A. RIS-assisted Channel Modeling

To simplify the notation, m-th RIS is written as RIS(m). Then, we consider a Rayleigh fading environment such that the small-scale fading channels between the BS-RIS(m) and the user-RIS(m) are denoted by $\tilde{\boldsymbol{H}}_{k,m} = [\boldsymbol{h}_{k,m,1}, \boldsymbol{h}_{k,m,2}, ..., \boldsymbol{h}_{k,m,I}] \in \mathbb{C}^{n\times I}$ and $\tilde{\boldsymbol{g}}_{k,m}^T = [g_{k,m,1}, g_{k,m,2}, ..., g_{k,m,I}]^T \in \mathbb{C}^{I\times 1}$, respectively. To account for correlation among transmit antenna elements, we adopt a separable (or Kronecker) correlation model, as proposed in [38], for analytical tractability. Consequently, the channel matrix can be expressed as:

$$\boldsymbol{H}_{k,m} = \tilde{\boldsymbol{H}}_{k,m}\boldsymbol{R}^{\frac{1}{2}}, \tag{1}$$

where $\tilde{\boldsymbol{H}}_{k,m} \in \mathbb{C}^{n\times I}$ contains i.i.d. circularly-symmetric complex Gaussian random variables, with zero mean and unit variance. The term $\boldsymbol{R} \in \mathbb{C}^{I\times I}$ represents the non-singular transmit correlation matrix, defined as $\boldsymbol{R} = \mathbb{E}[\boldsymbol{H}_{k,m}^{\dagger}\boldsymbol{H}_{k,m}]$. It is assumed that all users experience the same transmit correlation for simplicity and analytical tractability. Furthermore, the channel vector between the user and the m-th RIS is expressed as $\boldsymbol{g}_{k,m} = \tilde{\boldsymbol{g}}_{k,m}\boldsymbol{R}^{\frac{1}{2}} \in \mathbb{C}^{1\times I}$. Let $\boldsymbol{\phi}_{k,m} = [\phi_{k,m,1}, \phi_{k,m,2}, ..., \phi_{k,m,I}]^T$ is the phase shifts introduced by the m-th RIS and the i-th reflecting coefficient of the RIS(m) is expressed as $\phi_{k,m,i} = \beta_{k,m,i}e^{j\omega_{k,m,i}}$ with $\beta_{k,m,i} \in [0,1]$ and $\omega_{k,m,i}$ accounts for the reflecting amplitude and phase rotation of the RIS(m), respectively. Thus, the cascaded BS-RIS(m)-user channel $\boldsymbol{u}_{k,m}$ is represented as

$$\boldsymbol{u}_{k,m} = \boldsymbol{\phi}_{k,m}^T \mathrm{diag}\{\boldsymbol{g}_{k,m}\}\boldsymbol{H}_{k,m} = \boldsymbol{\phi}_{k,m}^T\boldsymbol{V}_{k,m}, \tag{2}$$

where $\boldsymbol{V}_{k,m} = \mathrm{diag}\{\boldsymbol{g}_{k,m}\}\boldsymbol{H}_{k,m}$ is the cascaded channel at the k-th UE and only depends on the downlink CSI.

B. Data Transmission

We assume that the small-scale fading channel is considered to be the direct BS-user k link, which is denoted as $\boldsymbol{h}_k$. By utilizing transmit beamforming of the BS $\boldsymbol{W}_k \in \mathbb{C}^{n\times n}$, the transmit signal can be written as $\boldsymbol{s}_k = \boldsymbol{W}_k^H\boldsymbol{x}_k$, where $\boldsymbol{x}_k = [x_{1,k}, ..., x_{i,k}, ...x_{n,k}]$ is the transmit signal of the k-th user with average unit power, i.e., $\mathbb{E}[|x_{i,k}|^2] = 1$. $\boldsymbol{x}_k$ should satisfy power constraint $\mathbb{E}[||\boldsymbol{W}_k||^2] = p_k$. Thus, combining the multiple RISs with the cascaded channel model in (2), the received pilot signal of k-th user from M RIS is expressed as

$$\hat{\mathrm{y}}_k = \sqrt{p_k}\left(\boldsymbol{h}_k^T + \sum_{m=1}^{M}\boldsymbol{\phi}_{k,m}^T\boldsymbol{V}_{k,m}\right)\boldsymbol{s}_k + n_k, \tag{3}$$

where $\boldsymbol{h}_k \in \mathbb{C}^{n\times 1}$ represents the direct link between the BS and user; $n_k \sim \mathcal{CN}(0,\sigma^2)$ denotes the noise at the k-th user.

To facilitate the multiple RISs design, the wake-up communication scheduling approach is developed, which has been widely used in wireless communication [39], [40]. Define the indicator variables $\Im_{k,0}$ and $\Im_{k,m}$ represent the activity status of the direct and m-th reflected links, respectively. Specifically, the direct channel serves the user if $\Im_{k,0} = 1$, otherwise, $\Im_{k,0} = 0$. Similarly, if $\Im_{k,m} = 1$, the m-th reflected channel migrates the signal to the user, while no signal is transmitted if $\Im_{k,m} = 0$. Based on these definitions, the following scheduling constraints can be established

$$\Im_{k,0} \le 1, \quad \Im_{k,0} \in \{0,1\}, \tag{6}$$

$$\Im_{k,m} \le 1, \quad \Im_{k,m} \in \{0,1\}, m = 1, .., M \tag{7}$$

where the indicator $\Im$ could represent whether the active RIS components are in wake-up or sleep mode for a given user or service. When $\Im = 1$, the RIS is actively reflecting and

$$\mathrm{y}_{k,0} = \underbrace{\sqrt{p_{k,0}}\mathbb{E}\left\{\|\boldsymbol{h}_k\|\right\}}_{\Delta_{DS_{k,0}}} s_{k,0} + \underbrace{\sqrt{p_{k,0}}\left(\|\boldsymbol{h}_k\| - \mathbb{E}\left\{\|\boldsymbol{h}_k\|\right\}\right)}_{\Delta_{SI_{k,0}}} s_{k,0} + \underbrace{\sum_{\substack{i=1,\\ i\neq k}}^{K} \sqrt{p_{i,0}}\left(\frac{\boldsymbol{h}_i^* \boldsymbol{h}_i}{\|\boldsymbol{h}_i\|}\right)}_{\mathbb{I}_{i\to k,0}} s_{k,0} + \hat{n}_{k,0}, \tag{4}$$

$$\mathrm{y}_{k,m} = \underbrace{\sqrt{p_{k,m}}\mathbb{E}\left\{\|\tilde{\boldsymbol{u}}_{k,m}\|\right\}}_{\Delta_{DS_{k,m}}} s_{k,m} + \underbrace{\sqrt{p_{k,m}}\left(\|\tilde{\boldsymbol{u}}_{k,m}\| - \mathbb{E}\left\{\|\tilde{\boldsymbol{u}}_{k,m}\|\right\}\right)}_{\Delta_{SI_{k,m}}} s_{k,m} + \underbrace{\sqrt{p_{k,m}}\sum_{\substack{i=1,\\ i\neq k}}^{K} \left(\frac{\tilde{\boldsymbol{u}}_{i,m}\tilde{\boldsymbol{u}}_{i,m}^*}{\|\tilde{\boldsymbol{u}}_{i,m}\|}\right)}_{\mathbb{I}_{i\to i,m}} s_{k,m} + \hat{n}_{k,m} \tag{5}$$

amplifying the signal for the intended user. When $\Im = 0$, the RIS is in sleep mode or not actively participating in the signal's propagation.

C. Problem Formulation

Considering CPU computational load for the high-performance of system, we assume that the direct channel $\boldsymbol{h}_k$ is blocked, and CPU is performed to awaken multiple RISs for providing the reflected links. Assuming that each user has knowledge of only the channel statistics, rather than the instantaneous channel gain, the received signal y_k at the k-th user consists of the superposition of the direct signal and the reflected signal, which can be written as

$$\mathrm{y}_k = \Im_{k,0}\mathrm{y}_{k,0} + (1 - \Im_{k,0}) \sum_{m=1}^{M} \Im_{k,m}\mathrm{y}_{k,m}, \tag{8}$$

where the direct signal $\mathrm{y}_{k,0}$, the reflected signal $\mathrm{y}_{k,m}$ are denoted by (4), (5) at the top of this page, $p_{k,0}$ and $p_{k,m}$ denote the transmission power of direct and m-th reflected channel for the k-th user, $\tilde{\boldsymbol{u}}_{k,m} = \boldsymbol{\phi}_{k,m}^T \boldsymbol{v}_{k,m}$, $\Delta_{DS_{k,0}}$, $\Delta_{DS_{k,m}}$ are the desired signal from direct channel and reflected channels, respectively. $\Delta_{SI_{k,0}}$, $\Delta_{SI_{k,m}}$ are the self-interference signal from direct channel and reflected channels, respectively. $\mathbb{I}_{i\to k,0}$, $\mathbb{I}_{i\to k,m}$ pertains to interference of direct signal and reflected signal from the i-th user and the k-th user, respectively. $\hat{n}_{k,0}$ and $\hat{n}_{k,m}$ represent the additive white Gaussian noise for the direct channel and the m-th reflected channel of the k-th user, respectively. When $\Im_{k,0} = 1$, the direct channel is activated to transmit the signal via the BS-user link. On the other hand, if $\Im_{k,m} = 1$, the reflected channels are awakened to transmit the signal with the BS-RIS-user channel.

Based on the above definitions, we assume that the direct and reflected channels are considered independent. When the direct channel is activated to transmit the signal via the BS-user link, the instantaneous signal-to-interference-plus-noise ratio (SINR) for the k-th user can be expressed as

$$\gamma_{k,0} = \frac{\left|\Delta_{DS_k,0}\right|^2}{\left|\Delta_{SI_k,0}\right|^2 + \sum_{\substack{i=1\\ i\neq k}}^{K} \left|\mathbb{I}_{i\to k,0}\right|^2 + \sigma_0^2}. \tag{9}$$

Thus, the corresponding ergodic downlink achievable rate of the k-th user is given by

$$R_{k,0} = \mathbb{E}\left\{\log_2\left(1 + \gamma_{k,0}\right)\right\}, \tag{10}$$

where $\mathbb{E}\{\cdot\}$ represents the expectation taken with respect to the small-scale channel fading. However, obtaining a closed-form expression for $R_{k,0}$ is challenging due to the complexity of deriving its probability distribution. To overcome this difficulty, an approximation result is proposed, as outlined in the following theorem.

Theorem 1. *[40] For any i, $j > 1$, if the distribution variance of positive random variables A and B is small, the following approximation result holds*

$$\mathbb{E}\left\{\log_2\left(1 + \frac{iA}{jB+1}\right)\right\} \approx \log_2\left(1 + \frac{\mathbb{E}\left\{iA\right\}}{\mathbb{E}\left\{jB\right\}+1}\right). \tag{11}$$

By applying Theorem 1, a lower bound for the ergodic rate (10) with $\zeta_{k,0} = 1$ can be derived as

$$R_{k,0} = \log_2\left(1 + \frac{\mathbb{E}\left\{\left|\Delta_{DS_k,0}\right|^2\right\}}{\mathbb{E}\left\{\left|\Delta_{SI_k,0}\right|^2 + \sum_{\substack{i=1\\ i\neq k}}^{K} \left|\mathbb{I}_{i\to k,0}\right|^2\right\} + \sigma_0^2}\right). \tag{12}$$

On the other hand, if the m-th RIS are awakened to transmit the signal with the BS-RIS-user channel, the instantaneous SINR at the k-th user can be expressed as

$$\gamma_{k,m} = \frac{\left|\Delta_{DS_k,m}\right|^2}{\left|\Delta_{SI_k,m}\right|^2 + \sum_{\substack{i=1\\ i\neq k}}^{K} \left|\mathbb{I}_{i\to k,m}\right|^2 + \sigma_m^2}. \tag{13}$$

Similarly, by applying Theorem 1, the ergodic downlink achievable rate of k-th user with $\zeta_{k,m} = 1$ can be written as

$$R_{k,m} = \log_2\left(1 + \frac{\mathbb{E}\left\{\left|\Delta_{DS_k,m}\right|^2\right\}}{\mathbb{E}\left\{\left|\Delta_{SI_k,m}\right|^2 + \sum\limits_{\substack{i=1\\ i\neq k}}^{K} \left|\mathbb{I}_{i\to k,m}\right|^2\right\} + \sigma_m^2}\right). \tag{14}$$

For the considered system, we aim to jointly design the transmit power, communication scheduling and phase shifts of multiple RISs to maximize the integrated throughput of the system. This optimization is subject to the transmit power constraint of the BS and the communication scheduling requirements of both the direct and reflected elements. To ensure fairness and provide users with a comparable quality of service

(QoS), our objective is to maximize the minimum ergodic rate lower bound among users by simultaneously optimizing the transmit power, communication scheduling, and phase shifts. However, it is evident that the max-min fairness approach may not fully meet the minimum QoS requirements for all users. To address this issue, if the QoS requirements remain unmet after solving the initial optimization problem, users with specific metrics, such as the weakest channel gain, will be excluded. The optimization is then repeated with the remaining users, allocating more resources to them [41]. This iterative approach is defined by the following problem.

$$\mathcal{P}0: \max_{\substack{\sum_{m=0}^{M} p_{k,m}, \boldsymbol{\phi}_m, \\ \{\zeta_{k,m}\}_{m=0}^{M}}} \min_{k} \sum_{k=1}^{K} \left\{ \Im_{k,0} \boldsymbol{R}_{k,0} + (1-\Im_{k,0}) \sum_{m=1}^{M} \Im_{k,m} \boldsymbol{R}_{k,m} \right\} \tag{15a}$$

$$s.t. \quad \phi_{k,m,i} \in \mathcal{F}, \tag{15b}$$

$$0 \le \sum_{k=1}^{K} \sum_{m=0}^{M} p_{k,m} \le P_{\max}, \tag{15c}$$

$$(6), (7) \tag{15d}$$

where (15b) prescribes the format of the RIS phase shift matrix, e.g., $\mathcal{F} = \{\phi_{k,m,i} | \phi_{k,m,i} = \beta_{k,m,i} e^{j\omega_{k,m,i}}, \omega_{k,m,i} \in [0, 2\pi)\}$, (15c) represents the transmit power constraints that no more than the maximum value $P_{\max}$.

Note that directly addressing the problem (15) presents significant challenges. These difficulties arise primarily from the self-interference term constraint and the complexity involved in deriving its probability distribution. To overcome these obstacles, we reformulate the objective function (15a) using the approach outlined in the following proposition.

Proposition 1. *Consider the ergodic rate $R_{k,0}$ in (12) and $R_{k,m}$ in (14), which can be written as follows*

$$R_{k,0} = \log_2 \left(1 + \frac{\frac{\pi}{4} \varrho_0 p_{k,0} \upsilon_k}{\varrho_k \upsilon_k W_{k,0} + \sigma_0^2} \right), \tag{16}$$

$$R_{k,m} = \log_2 \left(1 + \frac{\frac{\beta_0 \pi \phi_{k,m}}{4} p_{k,m} \chi_{k,m}}{\beta_0 \chi_{k,m} \phi_{k,m} W_{k,m} + \sigma_m^2} \right), \tag{17}$$

where $W_{k,0} = \alpha p_{k,0} + \sum_{u \neq k} p_{u,0}$, $W_{k,m} = \alpha p_{k,m} + \sum_{u \neq k} p_{u,m}$ are the interference power for the direct and reflected channels of the k-th user, respectively; α is a constant equal to $1 - \pi/4$, $\mathbb{E}\left\{ \|\tilde{\boldsymbol{h}}_k\| \right\} = \sqrt{\frac{\varrho_0 \upsilon_k \pi}{4}}$ and $\mathbb{E}\left\{ \|\tilde{\boldsymbol{u}}_{k,m}\| \right\} = \sqrt{\frac{\beta_0 \chi_{k,m} \phi_{k,m} \pi}{4}}$.

Proof: For the BS-RIS-user channel, we assume that channels of different RISs are independent. By exploiting the linear property of expectation, we have

$$\begin{aligned} &\mathbb{E}\left\{ \left| \Delta_{SI_{k,r}} \right|^2 + \sum_{j \neq k}^{K} \left| \mathbb{I}_{j \to k,r} \right|^2 \right\} \\ &= \mathbb{E}\left\{ \left| \Delta_{SI_{k,r}} \right|^2 \right\} + \mathbb{E}\left\{ \sum_{j \neq k}^{K} \left| \mathbb{I}_{j \to k,r} \right|^2 \right\}. \end{aligned} \tag{18}$$

We assume the fact that given $\mathbb{E}\{\|\tilde{\boldsymbol{u}}_{k,m}\|\} \sim \mathcal{CN}(0, \beta_0 \chi_{k,m} \phi_{k,m})$, $\|\tilde{\boldsymbol{u}}_{k,m}\|$ has Rayleigh distribution; then, the $\mathbb{E}\left\{ \left| \Delta_{SI_{k,r}} \right|^2 \right\}$ is derived as follows.

$$\begin{aligned} &\mathbb{E}\left\{ \left| \Delta_{SI_{k,r}} \right|^2 \right\} \\ &= \mathbb{E}\left\{ \left| \sqrt{p_{k,m}} \left(\|\tilde{\boldsymbol{u}}_{k,m}\| - \mathbb{E}\{\|\tilde{\boldsymbol{u}}_{k,m}\|\} \right) \right|^2 \right\} \\ &= \sum_{m=1}^{M} p_{k,m} \mathbb{E}\left\{ \left(\|\tilde{\boldsymbol{u}}_{k,m}\| - \mathbb{E}\{\|\tilde{\boldsymbol{u}}_{k,m}\|\} \right)^2 \right\} \\ &\overset{(a)}{=} \alpha p_{k,m} \beta_0 \chi_{k,m} \phi_{k,m}. \end{aligned} \tag{19}$$

where (a) is from the fact that $\mathbb{E}\{\|\tilde{\boldsymbol{u}}_{k,m}\|\} = \sqrt{\frac{\beta_0 \chi_{k,m} \pi}{4}}$ and $\alpha = 1 - \pi/4$. On the other hand, we investigate the second term

$$\begin{aligned} \mathbb{E}\left\{ \sum_{j \neq k}^{K} \left| \mathbb{I}_{j \to k,r} \right|^2 \right\} &= \mathbb{E}\left\{ \sum_{j \neq k}^{K} \left| \sqrt{p_{j,m}} \frac{\tilde{\boldsymbol{u}}_{k,m} \tilde{\boldsymbol{u}}_{j,m}^*}{\|\tilde{\boldsymbol{u}}_{j,m}\|} \right|^2 \right\} \\ &= \sum_{j \neq k}^{K} p_{j,m} \mathbb{E}\left\{ \|\tilde{\boldsymbol{u}}_{k,m}\|^2 \right\} \mathbb{E}\left\{ \left| \frac{\tilde{\boldsymbol{u}}_{j,m}}{\|\tilde{\boldsymbol{u}}_{j,m}\|} \right|^2 \right. \\ &\overset{(a)}{=} \sum_{j \neq k}^{K} p_{j,m} \mathbb{E}\left\{ \|\tilde{\boldsymbol{u}}_{k,m}\|^2 \right\} \\ &= \beta_0 \chi_{k,m} \phi_{k,m} \sum_{j \neq k}^{K} p_{j,m}, \end{aligned} \tag{20}$$

where (a) is from the $\frac{\tilde{\boldsymbol{u}}_{j,m}}{\|\tilde{\boldsymbol{u}}_{j,m}\|}$ that are independent random variables and $\mathbb{E}\left\{ \left| \frac{\tilde{\boldsymbol{u}}_{j,m}}{\|\tilde{\boldsymbol{u}}_{j,m}\|} \right|^2 \right\} = 1$.

By substituting (19) and (20) into (14), and defining $W_{k,m} = \alpha p_{k,m} + \sum_{j \neq k} p_{j,m}$, the proof of (17) is completed. Meanwhile, for the BS-user channel, the proof procedure of (16) is also deduced by assuming the fact that given $\mathbb{E}\left\{ \|\tilde{\boldsymbol{h}}_k\| \right\} = \sqrt{\frac{\varrho_0 \upsilon_k \pi}{4}}$.

Thus, the proof is completed. ■

III. Proposed Alternating Optimization Approach

As mentioned above, multiple variables in resolving problem $\mathcal{P}0$ to be optimized jointly, which lead to intractable to achieve the feasible solution, especially for high dimensional matrix and non-convex constraints. Based on this, a sum rate maximization (SRM) algorithm is employed, in which the phase shifts of multiple RISs, power allocation and the communication scheduling are optimized in an alternating fashion as follows.

A. Power Allocation Optimization

To promote fairness and ensure that all users experience a comparable quality of service (QoS), it is crucial to optimize the transmission power with the objective of maximizing the minimum ergodic rate lower bound among users. Thus, we optimize the transmit powers given the RISs' locations, and rewrite the problem $\mathcal{P}0$ as

$$\mathcal{P}1.1: \max_{p_{k,m}} \min_{k} \left\{ \Im_{k,0} \boldsymbol{R}_{k,0} + (1-\Im_{k,0}) \sum_{m=1}^{M} \Im_{k,m} \boldsymbol{R}_{k,m} \right\} \tag{21a}$$

$$s.t.\ \sum_{k=1}^{K}\sum_{m=0}^{M} p_{k,m} \le P_{\max}, \tag{21b}$$

$$(16), (17). \tag{21c}$$

Given that maximizing $\log(1+x)$ is equivalent to maximizing $\log(x)$, the function (21c) is therefore reformulated as follows

$$R_{k,0} = \log_2\left(\frac{\frac{\pi}{4}\xi_{k,0}p_{k,0}}{\xi_k W_{k,0}+1}\right), \tag{22}$$

$$R_{k,m} = \log_2\left(\frac{\frac{\pi}{4}\vartheta_{k,m}p_{k,m}}{\vartheta_{m,k}W_{k,m}+1}\right), \tag{23}$$

and $\xi_{k,0} = \frac{\varrho_k \upsilon_k}{\sigma_0^2}$, $\vartheta_{k,m} = \frac{\beta_0 \chi_{m,k}\phi_{m,k}}{\sigma_m^2}$.

Since the objective functions in (22) and (23) are still a difficult to solve problem (21), we propose a reformulation based on the following proposition.

Proposition 2. *Let a, b be the minimum value of $\log_2\left(\xi_{k,0}p_{k,0}\right)+\frac{X_{k,0}}{\ln(2)}$ and $\log_2\left(\sum_{m=1}^{M}\Im_{k,m}\vartheta_{k,m}p_{k,m}\right)+\frac{X_{k,r}}{\ln(2)}$, the optimization problem $\mathcal{P}1.1$ can be expressed as the following equivalent optimization problem.*

$$\mathcal{P}1.2: \max_{p_{k,m}} \Im_{k,0}a + (1-\Im_{k,0})b \tag{24a}$$

$$s.t.\ (21b), \tag{24b}$$

$$X_{k,0} \le 0, X_{k,m} \le 0, \forall\, k = \{1,2,\cdots,K\}, \tag{24c}$$

$$\xi_{k,0}W_{k,0}+1 \le e^{-X_{k,0}}, \tag{24d}$$

$$\sum_{m=1}^{M}\Im_{k,m}(\vartheta_{k,\,m}W_{k,\,m}+1) \le e^{-X_{k,r}}, \tag{24e}$$

$$\log_2\left(\xi_{k,0}p_{k,0}\right)+\frac{X_{k,0}}{\ln(2)} \ge a, \tag{24f}$$

$$\log_2\left(\sum_{m=1}^{M}\Im_{k,m}\vartheta_{k,m}p_{k,m}\right)+\frac{X_{k,r}}{\ln(2)} \ge b. \tag{24g}$$

Proof: By introducing auxiliary variables as $e^{-X_{k,0}} = \xi_{k,0}W_{k,0}+1$ and $e^{-X_{k,r}} = \sum_{m=1}^{M}\Im_{k,m}(\vartheta_{k,m}W_{k,m}+1)$, thus, the problem $\mathcal{P}1.2$ is reformulated as

$$\max_{\substack{p_{k,m},\\ X_{k,m},X_{k,m}}} \min_{k} \left\{\log_2\left(\sum_{m=1}^{M}\Im_{k,m}\vartheta_{k,m}p_{k,m}\right)\xi_{k,0}p_{k,0} + \frac{\Im_{k,0}(X_{k,0}-X_{k,m})+X_{k,m}}{\ln(2)}\right\} \tag{25a}$$

$$s.t.\ (21b) \tag{25b}$$

$$X_{k,0} \le 0, X_{k,m} \le 0, \forall\, k = \{1,2,\cdots,K\}, \tag{25c}$$

$$\xi_{k,0}W_{k,0}+1 \le e^{-X_{k,0}}, \tag{25d}$$

$$\sum_{m=1}^{M}\Im_{k,m}(\vartheta_{k,\,m}W_{k,m}+1) \le e^{-X_{k,r}}. \tag{25e}$$

To simplify the optimization process, we drop the additive term $\log_2(\pi/4)$ from (22) and (23), since it is a constant and does not affect the optimization result. To solve the max-min problem $\mathcal{P}1.1$, we introduce another auxiliary variable as $\Im_{k,0}a + (1-\Im_{k,0})b = \min_k\left(\log_2\left(\sum_{m=1}^{M}\Im_{k,m}\vartheta_{k,m}p_{k,m}\right)\xi_{k,0}p_{k,0} + \frac{\Im_{k,0}(X_{k,0}-X_{k,m})+X_{k,m}}{\ln(2)}\right)$. By substituting $\Im_{k,0}a + (1-\Im_{k,0})b$ in (25a), $\mathcal{P}1.1$ is reformulated as the problem (24), thereby completing the proof. ∎

In this reformulated problem, the objective function becomes affine, while constraints (24b) and (24c) form convex sets. It is worth noting that the term $\sum_{m=1}^{M}\Im_{k,m}\vartheta_{k,m}p_{k,m}$ is a concave function of $p_{k,m}$ and sum of concave functions remains concave. Moreover, the logarithm of a concave function is also concave, ensuring that (24f) and (24g) constitute convex sets as well. To handle the non-convex constraints (24d) and (24e), we introduce Lemma 1, which replaces these constraints with convex alternatives, enabling effective optimization.

Lemma 1. *By employing SRM, constraints (24d) and (24g) are replaced with the following convex constraints.*

$$\xi_{k,0}W_{k,0}+1 \le e^{-\bar{X}_{k,0}^{(t)}} - e^{-\bar{X}_{k,0}}\left(X_{k,0}-\bar{X}_{k,0}^{(t)}\right), \tag{26}$$

$$\sum_{m=1}^{M}\Im_{k,m}(\vartheta_{k,m}W_{k,m}+1) \le e^{-\bar{X}_{k,r}^{(t)}} - e^{-\bar{X}_{k,r}}\left(X_{k,r}-\bar{X}_{k,r}^{(t)}\right). \tag{27}$$

Proof: Since the direct path and RIS-assisted reflection paths are independent, the constraints (24d) and (24e) of Lemma 1 can be proved separately. For the direct path case (26), it is important to note that $e^{-X_{k,0}}$ is a convex function of $X_{k,0}$. As a result, the first-order Taylor expansion of $e^{-X_{k,0}}$ at any point provides a global lower bound for this function. Consequently, we replace the right-hand side of (24d) with the Taylor expansion evaluated around the point $\bar{X}_{k,0}$. Similarly, for the RIS-assisted reflection paths case, the same principle is applied to (27), establishing the corresponding result. ∎

Building on this, and using the insights from **Proposition 2** and **Lemma 1**, a convex approximation of the problem $\mathcal{P}1.2$ at the t-th iteration can be reformulated as follows

$$\mathcal{P}1.3: \max_{p_{k,m},X_{k,0},X_{k,m}} \Im_{k,0}a + (1-\Im_{k,0})b, \tag{28a}$$

$$s.t.\ (24b), (24c), (24f), (24g) \tag{28b}$$

$$\xi_{k,0}W_{k,0}+1 \le e^{-\bar{X}_{k,0}^{(t)}} - e^{-\bar{X}_{k,0}}\left(X_{k,0}-\bar{X}_{k,0}^{(t)}\right), \tag{28c}$$

$$\sum_{m=1}^{M}\Im_{k,m}(\vartheta_{k,m}W_{k,m}+1) \le e^{-\bar{X}_{k,r}^{(t)}} - e^{-\bar{X}_{k,r}}\left(X_{k,r}-\bar{X}_{k,r}^{(t)}\right). \tag{28d}$$

The values of $\bar{X}_{k,0}^{(t)}$, $\bar{X}_{k,r}^{(t)}$ are computed using the Taylor expansion, where they are initialized as the optimal values obtained from solving $\mathcal{P}1.3$ in the $(t-1)$ th iteration. This iterative process is repeated until convergence is achieved. The steps of the proposed iterative algorithm for solving the power allocation subproblem are outlined in Algorithm 1.

B. Phase shifts of multiple RISs optimization

The design of phase shifts in multiple RISs is crucial in determining the performance of the multiple RIS-assisted

Algorithm 1 Power Allocation for Solving $\mathcal{P}1.3$

Require: $p_{k,m}$, $\phi_{k,m}$, $1 \le m \le M$, $1 \le k \le K$
1: **Initialization**:$X_{k,0}^{(0)} = -\ln(\sum_{m=1}^{M} \xi_{m,\,k} W_{m,\,k} + 1)$, $t = 1$, $\epsilon = 10^{-3}$
2: **Repeat**
3: Update: $\{p_{k,m}, X_{k,0}, X_{k,m}\}$ by solving the problem $\mathcal{P}1.3$
4: Update: $\{p_{k,m}^{(t+1)}\} = \{p_{k,m}^{(t)}\}$
5: Update: $X_{k,0}^{(t+1)} = X_{k,0}^{(t)}$
6: Update: $X_{k,m}^{(t+1)} = X_{k,m}^{(t)}$
7: **Next iteration:**
8: $t \leftarrow t + 1$
9: **Until**: $\left| \frac{\min_k R_k^{(t)} - \min_k R_k^{(t-1)}}{\min_k R_k^{(t-1)}} \right| \le \epsilon$

communication. Note that the achievable rate $R_{k,0}$ is irrelevant to phase shift design, and therefore can be ignored. Thus, we formulate the phase shifts of RIS sub-problem by maximizing the estimated composite channel gain, which is equivalent to the following maximization problem:

$$\max_{\boldsymbol{\phi}_{k,m},\, m=1,\ldots,M} \sum_{k=1}^{K} \left(\boldsymbol{h}_k + \sum_{m=1}^{M} \boldsymbol{\phi}_{k,m}^T \boldsymbol{V}_{k,m} \right)^2 \tag{29a}$$

$$s.t.\;\; \phi_{k,m,i} = \beta_{k,m,i} e^{j\omega_{k,m,i}}, \quad i = 1, ..., I \tag{29b}$$

$$\omega_{k,m,i} \in (0, 2\pi]. \tag{29c}$$

The above mentioned problem (29) is a complicated non-convex problem since $\sum_{k=1}^{K} \left(\boldsymbol{h}_k + \sum_{m=1}^{M} \boldsymbol{\phi}_{k,m}^T \boldsymbol{V}_{k,m} \right)^2$ is a non-concave function with respect to $\boldsymbol{\phi}_{k,m}$ [42]. To address this non-convex optimization problem, we define $\Upsilon_m \triangleq \left(\boldsymbol{h}_k + \sum_{m=1}^{M} \boldsymbol{\phi}_{k,m}^T \boldsymbol{V}_{k,m} \right)^2$, so that the objective function (29a) can be rewritten as

$$\begin{aligned} \Upsilon_m &= \left\| \boldsymbol{h}_k^T + \sum_{m=1}^{M} \boldsymbol{\phi}_{k,m}^T \boldsymbol{V}_{k,m} \right\|^2 \\ &= \left(\boldsymbol{h}_k^T + \sum_{m=1}^{M} \boldsymbol{\phi}_{k,m}^T \boldsymbol{V}_{k,m} \right)^H \left(\boldsymbol{h}_k^T + \sum_{m=1}^{M} \boldsymbol{\phi}_{k,m}^T \boldsymbol{V}_{k,m} \right) \\ &= \left(\sum_{m=1}^{M} \boldsymbol{\phi}_{k,m}^T \boldsymbol{V}_{k,m} \right)^H \left(\sum_{m=1}^{M} \boldsymbol{\phi}_{k,m}^T \boldsymbol{V}_{k,m} \right) + \|\boldsymbol{h}_k\|^2 + \\ &\quad 2\mathrm{Re}\left\{ \boldsymbol{h}_k^T \left(\sum_{m=1}^{M} \boldsymbol{\phi}_{k,m}^T \boldsymbol{V}_{k,m} \right) \right\}. \end{aligned} \tag{30}$$

The first term in (30) can be further expressed as

$$\begin{aligned} &\left(\sum_{m=1}^{M} \boldsymbol{\phi}_{k,m}^T \boldsymbol{V}_{k,m} \right)^H \left(\sum_{m=1}^{M} \boldsymbol{\phi}_{k,m}^T \boldsymbol{V}_{k,m} \right) = \\ &\sum_{m=1}^{M} \sum_{i=1}^{I} \|\boldsymbol{v}_{k,m,i}\|^2 |\phi_{m,i}|^2 + \sum_{m=1}^{M} \sum_{i=1}^{I} \sum_{i \ne q}^{I} \left(\phi_{m,i}^T \boldsymbol{v}_{k,m,i} \boldsymbol{v}_{k,m,i}^T \phi_{m,i} \right), \end{aligned} \tag{31}$$

where $\boldsymbol{V}_{k,m} = [\boldsymbol{v}_{k,m,1}, \boldsymbol{v}_{k,m,2}, ..., \boldsymbol{v}_{k,m,I}]^T$ and $\boldsymbol{\phi}_{k,m} = [\phi_{k,m,1}, \phi_{k,m,2}, ..., \phi_{k,m,I}]^T$.

It follows that (31) has no phase information because of the definition of $\phi_{k,m,i}$ such that $|e^{j\omega_{k,m,i}}|^2 = 1$. Furthermore, there exist the cross terms in the second term of (31), which can be negligible with $2\mathrm{Re}\{\boldsymbol{h}_k(\sum_{m=1}^{M}\sum_{i=1}^{I} \phi_{k,m,i}^T \boldsymbol{v}_{k,m,i})\} >> \sum_{m=1}^{M}\sum_{i=1}^{I}\sum_{i\ne q}^{I}(\phi_{m,i}^T \boldsymbol{v}_{k,m,i} \boldsymbol{v}_{k,m,i}^T \phi_{m,i})$. To simplify the problem, we disregard the first term in (30) since it does not affect the optimization process. The remaining terms are independent of the phase shifts, allowing us to reformulate the maximization problem for the total channel gain as follows

$$\max_{\boldsymbol{\phi}_{k,m},\, m=1,\ldots,M} \sum_{k=1}^{K} \mathrm{Re}\left\{ \boldsymbol{h}_k^T \left(\sum_{m=1}^{M} \sum_{i=1}^{I} \phi_{k,m,i}^T \boldsymbol{v}_{k,m,i} \right) \right\}. \tag{32}$$

From the problem (32), the i-th reflecting coefficient in the m-th RIS can be determined by maximizing the approximate version of the total channel gain given by

$$\phi_{k,m,i} \approx \tan^{-1}\left(\frac{\mathrm{Im}(\sum_{k=1}^{K} \boldsymbol{h}_k^T \boldsymbol{v}_{k,m,i})}{\mathrm{Re}(\sum_{k=1}^{K} \boldsymbol{h}_k^T \boldsymbol{v}_{k,m,i})} \right). \tag{33}$$

To reduce the hardware complexity and overhead cost, we consider to quantify the phase shifts of the RIS elements. Let $\omega_{k,m,i} \triangleq \angle \phi_{k,m,i}$ and B be the quantization bits, the quantized phase $\bar{\omega}_{k,m,i}$ can be derived as follows

$$\bar{\omega}_{k,m,i} = \mathrm{round}\left(\frac{\omega_{k,m,i}}{\delta} \right) \times \delta, \tag{34}$$

where $\delta = \frac{2\pi}{2^B}$ indicates the resolution of phase shifts. Algorithm 2 summarizes the phase shifts optimization processing.

Algorithm 2 Phase shifts of RIS design

Require: $\beta_{k,m,i} = 1$, $1 \le k \le K$
1: Initialization:$\boldsymbol{h}_{k,m}$, $\boldsymbol{v}_{k,m}$
2: **repeat**
3: Update the variable $\omega_{k,m,i}$, by solving the problem (33)
4: Update $\bar{\omega}_{k,m,i}$ by solving (34)
5: **until** convergence
6: **Output**: $\bar{\omega}_{k,m,i}$, $i = 1, 2, .., I$

C. Communication Scheduling Optimization

To optimize the communication scheduling, the integer communication scheduling constraints (6) are relaxed into a form of continuous constraints as follows

$$\Im_{k,0} \le 1, \quad 0 \le \Im_{k,0} \le 1, \tag{35a}$$

$$\Im_{k,m} \le 1, \quad 0 \le \Im_{k,m} \le 1. \tag{35b}$$

For any given transmit power and phase shifts of multiple RISs, the communication scheduling subproblem is

$$\begin{aligned} \mathcal{P}3: \max_{\Im_{k,0}, \Im_{k,m}} \sum_{k=1}^{K} \Bigg\{ &\Im_{k,0} \log_2\left(\frac{\frac{\pi}{4}\xi_{k,0} p_{k,0}}{\xi_k W_{k,0} + 1} \right) + \\ &(1 - \Im_{k,0}) \sum_{m=1}^{M} \Im_{k,m} \log_2\left(\frac{\frac{\pi}{4}\vartheta_{k,m} p_{k,m}}{\vartheta_{k,m} W_{k,m} + 1} \right) \Bigg\} \end{aligned} \tag{36a}$$

$$s.t., (35a), (35b). \tag{36b}$$

It is conceivable that the objective function (36a) is a scalar continuously differentiable function. Therefore, by successively updating $\Im_{k,0}$ and $\Im_{k,m}$, it is not difficult to obtain a

locally optimal solution. It follows that the transmit power, phase shifts of multiple RISs and communication scheduling can be optimized by the alternate optimization. However, the relaxation of the binary constraints (6) and (7) into continuous constraints (35a) and (35b) is indeed an approximation that may lead to solutions that are not feasible for the original problem P_0. To tackle this issue, an additional step is introduced to map the continuous values back to binary values after solving the relaxed problem. This can be done using a thresholding method, where values closer to 1 are set to 1, and values closer to 0 are set to 0. This post-processing step would ensure that the final solution is feasible for the original problem P_0.

D. Complexity Analysis

This subsection presents a detailed complexity analysis, comparing the proposed algorithm with the exhaustive search method to highlight their computational efficiency and practicality. The exhaustive search method evaluates all possible combinations of phase shifts, power allocation, and communication scheduling. Each RIS consists of s reflecting elements, and the complexity of this approach grows exponentially with the number of elements. The total computational complexity is expressed as $\mathcal{O}(2^s I_{iter}(2KML^2 + KLM^2 + KML))$, where I_{iter} is the number of iterations and 2^s accounts for the iterations required to update the dual variables during the search process. As described above, the complexity of the exhaustive search method primarily arises from two sources: computing Algorithm 1 in the first step and linearly determining the phase shifts of multiple RISs in the second step. Consequently, the overall complexity is given by $\mathcal{O}(2^s I_{iter}(2KML^2 + KLM^n + KML))$. In contrast, the proposed algorithm strikes a better balance between computational complexity and system performance. This improvement is validated through the numerical results presented in the next section.

IV. Numerical Simulation

In this section, we present numerical results to assess the effectiveness and robustness of the proposed distributed RIS-assisted algorithm in terms of the SE of the considered system. Unless stated otherwise, the simulation parameters used for evaluation are outlined as follows. The number of scattering clusters and the propagation paths are set as $N_i = 8$ and $N_l = 10$, respectively. We also consider the variance of path gain for each cluster as $\sigma_{i,l}^2 = 0.1, \forall i, l$. All simulation results are based on Monte Carlo simulation, which are averaged over 5000 times. The Rayleigh fading channel is considered as a general channel to be generated with large-scale channel fading parameters [43]. To ensure a fair comparison, two types of benchmarks are provided as follows.

1) Zero-forcing with per-antenna power constraint (ZF-PPC): The ZF-PPC approach focuses on the power allocation problem of maximizing the SE by employing ZF precoding under per-antenna power constraint [44]. Considering that the optimization problem of ZF-PPC is a convex optimization problem, the iterative strategy is employed to implement ZF-PAC. It should be noted that the solution of the ZF-PPC approach would be unable to meet the power setting due to only single-antenna power constraint. Based on this, the power constraint is scaled down equivalently, for a fair comparison.

2) Adaptive Power Allocation Schemes (APAS): The APAS approach with adaptive power allocation is used as an optimal baseline in the simulation result. The performance of the APAS will be plotted to verify the impact of effective power allocation..

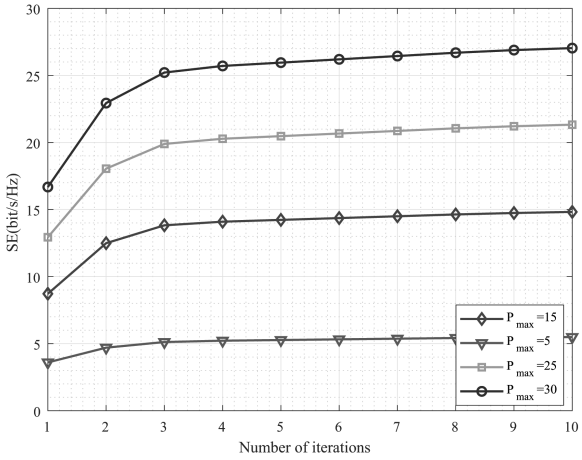

Fig. 2. Convergence behavior of our proposed algorithm.

A. Convergence Analysis

The convergence behavior of the considered RIS-assisted scheme is investigated, where jointly the communication scheduling, the phase shifts of multiple RISs, and power allocation are optimized to maximize system SE. As shown in Fig. 2, it seems that the proposed distributed RIS-assisted algorithm converges in less than 5 iterations under the small transmit power $P_{\max} = 5$ dBm case, while for a large transmit power $P_{\max} = 25$ dBm, only 8 iterations are required for reaching convergence. It is remarkable that when the number of iterations is larger than 10 times, the differences of SE value is slowly minor, which can almost be neglected. Therefore, the system throughput obtained by the different transmit power converges quickly, and, in general, only a small number of iterations is needed for ensuring the convergence. According to simulations, it is also noted that the SE value of the system increases as the power $P_{\max}$ increases.

B. Comparison of Different RISs

To further illustrate the performance of the proposed method, Fig. 3 shows the relationship between the achievable SE of the considered distributed RIS-assisted scheme and the number of multiple RISs. More specifically, as the number of RISs increases from 10 to 90, the achievable SE of the system approaches the Shannon limit. This improvement occurs because the addition of multiple RISs enhances the SE of the distributed RIS-assisted multiuser system, indicating that deploying multiple RISs can significantly boost system throughput. These observations verify the correctness of the proposed method.

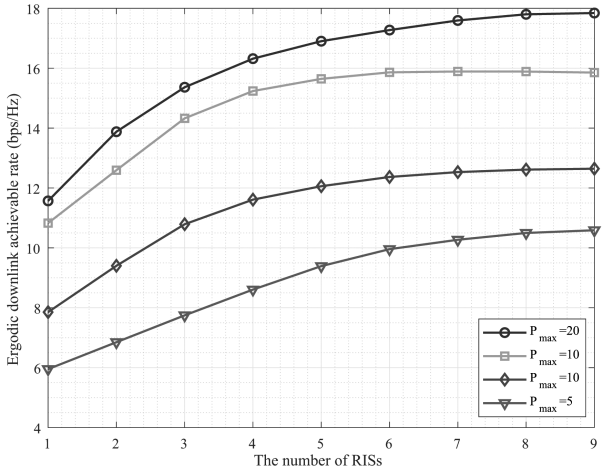

Fig. 3. The ergodic downlink achievable rate versus SNR levels with different number of multiple RISs.

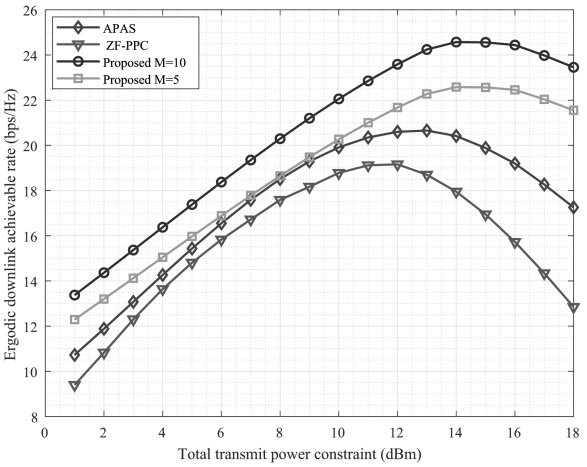

Fig. 4. The ergodic downlink achievable rate versus transmit power: $K = 10$, $N = 25$.

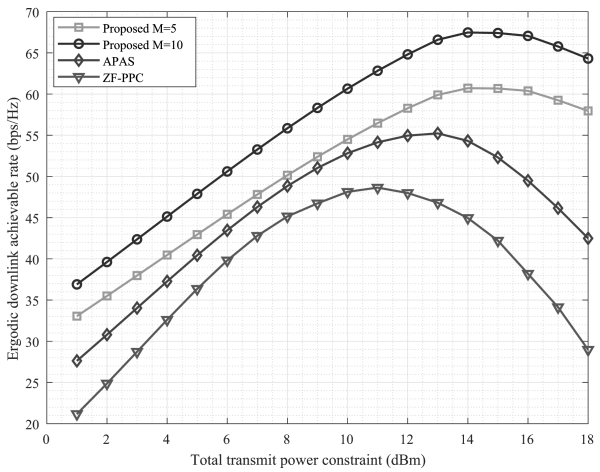

Fig. 5. The ergodic downlink achievable rate versus transmit power: $K = 25$, $N = 64$.

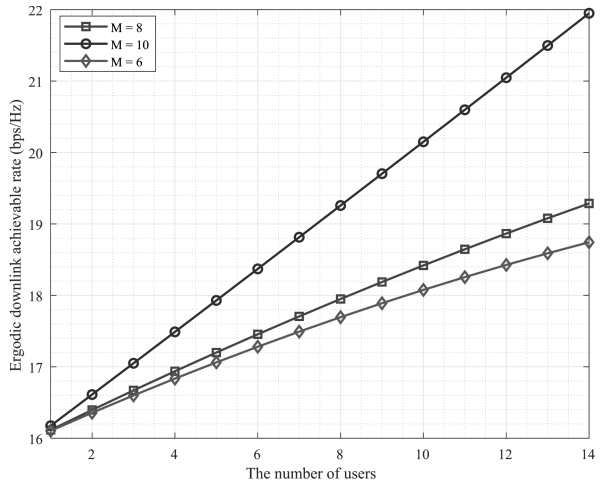

Fig. 6. The achievable sum rate versus the number of users K: $\gamma = \frac{1}{2}$.

Another notable observation is that the power consumption of the distributed RIS-assisted scheme decreases as the number of RIS reflecting elements increases. This trend occurs because a larger number of reflecting elements improves the achievable SE of the system through the proposed phase-shift control mechanism for multiple RISs. Moreover, it is evident that deploying more RISs results in substantial performance gains, highlighting the potential of the distributed RIS-assisted multiuser system as an effective solution to enhance overall system performance.

C. Comparison of Different Schemes

We evaluate the desired SE performance of the considered distributed RIS-assisted scheme. We set the number of users $K = \{10, 25\}$ and antennas $N = \{25, 49\}$. Figs. 4 and 5 show the achievable SE versus the total power constraint. It is noted that the APAS approach can achieve comparable performance to the proposed distributed RIS-assisted scheme, when the total power is close to $P_{\max} = 8$ dBm and $K = 10$, $N = 25$. This is because the achievable SE is degraded in the detrimental region, but the APAS approach cannot control the transmit power. Comparing ZF-PPC and APAS in Figs. 4 and 5, we can notice that the achievable SE can be further enhanced with power allocation proposed in Algorithm 1, which indicates that the distributed RIS-assisted scheme can be further improved to achieve high sum rate.

It can be intuitively concluded that achieving the desired performance for the ZF-PPC and APAS schemes comes at the cost of extremely high computational complexity. Furthermore, by comparing these figures from Figs. 4 and 5, we can observe that the considered distributed RIS-assisted scheme outperforms other baseline schemes in the large number of users cases. This is because the path loss between the BS and the user become more and more serious in a complicated environment, while multiple RISs can effectively compensate for this drawback, thereby improving the system throughput.

D. Comparison of Different Users

Finally, we investigate the relationship between the number of users K and the number of antennas N for the proposed

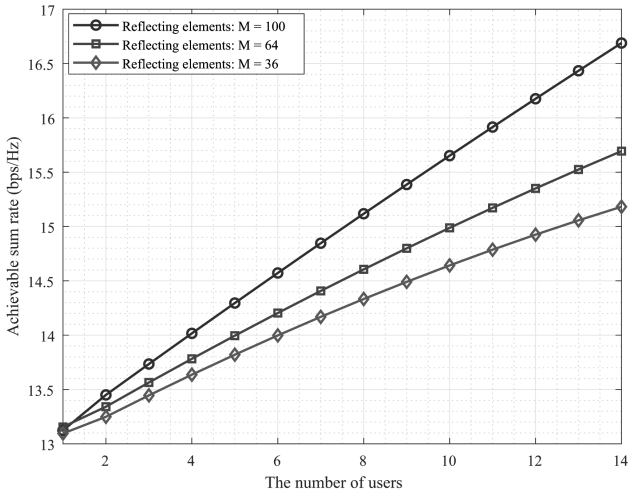

Fig. 7. The achievable sum rate versus the number of users K: $\gamma = \frac{3}{4}$

technique. In this setting, both K and N are increased while maintaining a fixed ratio $\gamma = \frac{K}{N}$. Figs. 6 and 7 show the achievable SE of the system with $\gamma = \frac{1}{2}$ and $\gamma = \frac{2}{3}$, respectively. Specifically, Fig. 6 depicts the achievable SE as a function of the number of users. As the number of users increases, the system's throughput improves due to the benefits of SE-oriented power allocation, which efficiently distributes resources to enhance performance. Building on the above analysis, we conclude that the joint design of power allocation, phase shifts of multiple RISs, and communication scheduling offers valuable insights for practical systems operating in rich macro-diversity cellular scenarios.

V. Conclusion

In this paper, we investigated distributed RIS-assisted multiuser systems, where multiple RISs are utilized to enhance signal transmission between the BS and users. To minimize the total power consumption of such systems, we formulated an optimization problem aimed at maximizing the ergodic achievable rate by jointly optimizing the phase shifts of multiple RISs, power allocation, and communication scheduling. To address this challenging problem, we first tackled the subproblem of power allocation, which was solved using the SRM-based iterative algorithm. Next, a minimization-maximization approach was employed to derive an approximate closed-form solution for the phase shifts of multiple RISs. Subsequently, effective iterative optimization techniques were applied to refine the communication scheduling. Simulation results demonstrated that the proposed distributed RIS-assisted algorithm significantly improves the total achievable SE compared to existing benchmark methods, highlighting its effectiveness and potential in enhancing system performance.

References

[1] W. Hao, G. Sun, M. Zeng, Z. Chu, Z. Zhu, O. A. Dobre, and P. Xiao, "Robust design for intelligent reflecting surface-assisted MIMO-OFDMA terahertz IoT networks," *IEEE Internet of Things Journal*, vol. 8, no. 16, pp. 13052–13064, 2021.

[2] S. Mao, L. Liu, N. Zhang, J. Hu, K. Yang, F. R. Yu, and V. C. M. Leung, "Intelligent reflecting surface-assisted low-latency federated learning over wireless networks," *IEEE Internet of Things Journal*, vol. 10, no. 2, pp. 1223–1235, 2023.

[3] X. Li, C. Zhang, C. He, G. Chen, and J. A. Chambers, "Sum-rate maximization in IRS-assisted wireless power communication networks," *IEEE Internet of Things Journal*, vol. 8, no. 19, pp. 14959–14970, 2021.

[4] A. Shojaeifard, K.-K. Wong, K.-F. Tong, Z. Chu, A. Mourad, A. Haghighat, I. Hemadeh, N. T. Nguyen, V. Tapio, and M. Juntti, "MIMO evolution beyond 5G through reconfigurable intelligent surfaces and fluid antenna systems," *Proceedings of the IEEE*, pp. 1–22, 2022.

[5] W. Xu, L. Gan, and C. Huang, "A robust deep learning-based beamforming design for RIS-assisted multiuser MISO communications with practical constraints," *IEEE Transactions on Cognitive Communications and Networking*, vol. 8, no. 2, pp. 694–706, 2022.

[6] C. Pan, H. Ren, K. Wang, M. Elkashlan, A. Nallanathan, J. Wang, and L. Hanzo, "Intelligent reflecting surface aided MIMO broadcasting for simultaneous wireless information and power transfer," *IEEE Journal on Selected Areas in Communications*, vol. 38, no. 8, pp. 1719–1734, 2020.

[7] B. Zheng, C. You, W. Mei, and R. Zhang, "A survey on channel estimation and practical passive beamforming design for intelligent reflecting surface aided wireless communications," *IEEE Communications Surveys Tutorials*, pp. 1–1, 2022.

[8] Z. Chen, L. Huang, H. C. So, H. Jiang, X. Y. Zhang, and J. Wang, "Deep Reinforcement Learning Over RIS-Assisted Integrated Sensing and Communication: Challenges and Opportunities," *IEEE Vehicular Technology Magazine*, pp. 2–10, 2024.

[9] J. Mirza and B. Ali, "Channel estimation method and phase shift design for reconfigurable intelligent surface assisted MIMO networks," *IEEE Transactions on Cognitive Communications and Networking*, vol. 7, no. 2, pp. 441–451, 2021.

[10] K. Fang, Y. Ouyang, B. Zheng, L. Huang, G. Wang, and Z. Chen, "Security Enhancement for RIS-Aided MEC Systems with Deep Reinforcement Learning," *IEEE Transactions on Communications*, pp. 1–1, 2024.

[11] H. Niu, Z. Chu, F. Zhou, Z. Zhu, L. Zhen, and K.-K. Wong, "Robust design for intelligent reflecting surface assisted secrecy SWIPT network," *IEEE Transactions on Wireless Communications*, vol. 21, no. 6, pp. 4133–4149, 2022.

[12] Y. Cang, M. Chen, J. Zhao, Z. Yang, Y. Hu, C. Huang, and K.-K. Wong, "Joint deployment and resource management for VLC-enabled RISs-assisted UAV networks," *IEEE Transactions on Wireless Communications*, vol. 22, no. 2, pp. 746–760, 2023.

[13] Z. Chen, Y. Guo, P. Zhang, H. Jiang, Y. Xiao, and L. Huang, "Physical Layer Security Improvement for Hybrid RIS-Assisted MIMO Communications," *IEEE Communications Letters*, vol. 28, no. 11, pp. 2493–2497, 2024.

[14] Z. Chen, J. Tang, X. Du, X. Zhang, D. K. C. So, and K.-K. Wong, "Joint energy and information beamforming design for RIS-assisted wireless powered communication," in *2022 IEEE 22nd International Conference on Communication Technology (ICCT)*, pp. 536–540, 2022.

[15] Y. Xu, Z. Gao, Z. Wang, C. Huang, Z. Yang, and C. Yuen, "RIS-enhanced WPCNs: Joint radio resource allocation and passive beamforming optimization," *IEEE Transactions on Vehicular Technology*, vol. 70, no. 8, pp. 7980–7991, 2021.

[16] A. Khalili, S. Zargari, Q. Wu, D. W. K. Ng, and R. Zhang, "Multi-objective resource allocation for IRS-aided SWIPT," *IEEE Wireless Communications Letters*, vol. 10, no. 6, pp. 1324–1328, 2021.

[17] X. Gu, W. Duan, G. Zhang, Y. Ji, M. Wen, and P.-H. Ho, "Socially aware V2X networks with RIS: Joint resource optimization," *IEEE Transactions on Vehicular Technology*, vol. 71, no. 6, pp. 6732–6737, 2022.

[18] S. Gong, C. Xing, X. Zhao, S. Ma, and J. An, "Unified IRS-aided MIMO transceiver designs via majorization theory," *IEEE Transactions on Signal Processing*, vol. 69, pp. 3016–3032, 2021.

[19] J. Du, F. R. Yu, G. Lu, J. Wang, J. Jiang, and X. Chu, "MEC-assisted immersive VR video streaming over terahertz wireless networks: A deep reinforcement learning approach," *IEEE Internet of Things Journal*, vol. 7, no. 10, pp. 9517–9529, 2020.

[20] J. Li, X. Li, Y. Bi, and J. Ma, "Energy-efficient joint resource allocation with reconfigurable intelligent surfaces in symbiotic radio networks," *IEEE Transactions on Cognitive Communications and Networking*, pp. 1–1, 2022.

[21] P. Mursia, V. Sciancalepore, A. Garcia-Saavedra, L. Cottatellucci, X. C. Prez, and D. Gesbert, "RISMA: Reconfigurable intelligent surfaces en-

abling beamforming for IoT massive access," *IEEE Journal on Selected Areas in Communications*, vol. 39, no. 4, pp. 1072–1085, 2021.

[22] Z. Chen, J. Tang, X. Zhang, Q. Wu, Y. Wang, D. K. C. So, S. Jin, and K.-K. Wong, "Offset learning based channel estimation for intelligent reflecting surface-assisted indoor communication," *IEEE Journal of Selected Topics in Signal Processing*, pp. 1–14, 2021.

[23] W. Jiang, Y. Zhang, J. Zhao, Z. Xiong, and Z. Ding, "Joint transmit precoding and reflect beamforming design for IRS-assisted MIMO cognitive radio systems," *IEEE Transactions on Wireless Communications*, vol. 21, no. 6, pp. 3617–3631, 2022.

[24] S. H. Hong, J. Park, S.-J. Kim, and J. Choi, "Hybrid beamforming for intelligent reflecting surface aided millimeter wave MIMO systems," *IEEE Transactions on Wireless Communications*, vol. 21, no. 9, pp. 7343–7357, 2022.

[25] Z. Chen, J. Tang, X. Y. Zhang, Q. Wu, G. Chen, and K.-K. Wong, "Robust hybrid beamforming design for multi-RIS assisted MIMO system with imperfect CSI," *IEEE Transactions on Wireless Communications*, pp. 1–13, 2022.

[26] Y. Liu, J. Zhao, M. Li, and Q. Wu, "Intelligent reflecting surface aided MISO uplink communication network: Feasibility and power minimization for perfect and imperfect CSI," *IEEE Transactions on Communications*, vol. 69, no. 3, pp. 1975–1989, 2021.

[27] H. Zhang, H. Liu, J. Cheng, and V. C. M. Leung, "Downlink energy efficiency of power allocation and wireless backhaul bandwidth allocation in heterogeneous small cell networks," *IEEE Transactions on Communications*, vol. 66, no. 4, pp. 1705–1716, 2018.

[28] G. Yang, Y. Liao, Y.-C. Liang, O. Tirkkonen, G. Wang, and X. Zhu, "Reconfigurable intelligent surface empowered device-to-device communication underlaying cellular networks," *IEEE Transactions on Communications*, vol. 69, no. 11, pp. 7790–7805, 2021.

[29] Y. Cao, T. Lv, W. Ni, and Z. Lin, "Sum-rate maximization for multi-reconfigurable intelligent surface-assisted device-to-device communications," *IEEE Transactions on Communications*, vol. 69, no. 11, pp. 7283–7296, 2021.

[30] J. Zuo, Y. Liu, Z. Qin, and N. Al-Dhahir, "Resource allocation in intelligent reflecting surface assisted NOMA systems," *IEEE Transactions on Communications*, vol. 68, no. 11, pp. 7170–7183, 2020.

[31] K. K. Nguyen, S. R. Khosravirad, D. B. da Costa, L. D. Nguyen, and T. Q. Duong, "Reconfigurable intelligent surface-assisted multi-UAV networks: Efficient resource allocation with deep reinforcement learning," *IEEE Journal of Selected Topics in Signal Processing*, vol. 16, no. 3, pp. 358–368, 2022.

[32] C. Pradhan, A. Li, L. Song, J. Li, B. Vucetic, and Y. Li, "Reconfigurable intelligent surface (RIS)-enhanced two-way OFDM communications," *IEEE Transactions on Vehicular Technology*, vol. 69, no. 12, pp. 16270–16275, 2020.

[33] Y. Zhao, W. Xu, H. Sun, D. W. K. Ng, and X. You, "Cooperative reflection design with timing offsets in distributed multi-RIS communications," *IEEE Wireless Communications Letters*, vol. 10, no. 11, pp. 2379–2383, 2021.

[34] Y. Zhao, W. Xu, X. You, N. Wang, and H. Sun, "Cooperative reflection and synchronization design for distributed multiple-RIS communications," *IEEE Journal of Selected Topics in Signal Processing*, vol. 16, no. 5, pp. 980–994, 2022.

[35] Y. Gao, J. Xu, W. Xu, D. W. K. Ng, and M.-S. Alouini, "Distributed IRS with statistical passive beamforming for MISO communications," *IEEE Wireless Communications Letters*, vol. 10, no. 2, pp. 221–225, 2021.

[36] T. N. Do, G. Kaddoum, T. L. Nguyen, D. B. da Costa, and Z. J. Haas, "Multi-RIS-aided wireless systems: Statistical characterization and performance analysis," *IEEE Transactions on Communications*, vol. 69, no. 12, pp. 8641–8658, 2021.

[37] G. Zhou, C. Pan, H. Ren, D. Xu, Z. Zhang, J. Wang, and R. Schober, "A Framework for Transmission Design for Active RIS-Aided Communication With Partial CSI," *IEEE Transactions on Wireless Communications*, vol. 23, no. 1, pp. 305–320, 2024.

[38] G. Geraci, A. Y. Al-nahari, J. Yuan, and I. B. Collings, "Linear precoding for broadcast channels with confidential messages under transmit-side channel correlation," *IEEE Communications Letters*, vol. 17, no. 6, pp. 1164–1167, 2013.

[39] H. Yang, J. Zhao, Z. Xiong, K.-Y. Lam, S. Sun, and L. Xiao, "Privacy-preserving federated learning for UAV-enabled networks: Learning-based joint scheduling and resource management," *IEEE Journal on Selected Areas in Communications*, vol. 39, no. 10, pp. 3144–3159, 2021.

[40] M. Hua, L. Yang, Q. Wu, and A. L. Swindlehurst, "3D UAV trajectory and communication design for simultaneous uplink and downlink transmission," *IEEE Transactions on Communications*, vol. 68, no. 9, pp. 5908–5923, 2020.

[41] H. Ahmadinejad and A. Falahati, "Spectral efficiency in non-terrestrial heterogeneous networks with spectrum underlay access," *Physical Communication*, vol. 46, no. 9, pp. 101–113, 2021.

[42] S. Zhang and R. Zhang, "Capacity characterization for intelligent reflecting surface aided MIMO communication," *IEEE Journal on Selected Areas in Communications*, vol. 38, no. 8, pp. 1823–1838, 2020.

[43] Z. Chen, L. Huang, S. Xia, B. Tang, M. Haardt, and X. Y. Zhang, "Parallel Channel Estimation for RIS-Assisted Internet of Things," *IEEE Transactions on Intelligent Transportation Systems*, vol. 25, no. 8, pp. 9762–9773, 2024.

[44] F. Boccardi and H. Huang, "Zero-forcing precoding for the MIMO broadcast channel under per-antenna power constraints," in *2006 IEEE 7th Workshop on Signal Processing Advances in Wireless Communications*, pp. 1–5, 2006.